

# Structural, Morphological and Theoretical Modeling Studies on Polymer Composites of Nano Crystalline Ceramic Superconductor $\text{GdBa}_2\text{Ca}_3\text{Cu}_4\text{O}_{10.5+\delta}$

Vinila V.S<sup>1</sup>, Jayakumari Isac<sup>2</sup>

<sup>1,2</sup>Centre for Condensed Matter, Department of Physics, CMS College, Kottayam, Kerala, India

**Abstract:** Ceramic powder synthesis as a field of materials processing is undergoing rapid expansion. Modern ceramics have huge applications in electronics, aerospace, automotive, medical, etc. Composite materials are attracting much interest for technical applications and fundamental research. The blending of different sorts of materials produces composite structures which can combine different material properties or may reveal novel properties not existing in the constituent phases. High temperature superconducting materials, like many other ceramics, are inherently brittle in nature and therefore pose problems in converting them into simple usable forms such as flexible wires, shapes, sheets etc. In this section the authors describes a method for the preparation of Gadolinium Barium Calcium Copper Oxide,  $\text{GdBa}_2\text{Ca}_3\text{Cu}_4\text{O}_{10.5+\delta}$  (GBCCO)- super conducting ceramic powder materials based on pre-calcinations of oxides. In order to show the viability of the proposed method, super-conducting powder was prepared in special furnace. By using the classical polymer processing of converting raw polymeric materials into finished products of desirable shape and macromolecular structure, morphology, polymer is blended with ceramic superconductor  $\text{GdBa}_2\text{Ca}_3\text{Cu}_4\text{O}_{10.5+\delta}$  to form a new product. The results are analyzed by X-ray Diffraction (XRD), SEM, and EDX. This product is analyzed, characterized and property studies are done and found to be useful in many applications. Young's moduli of the composites are calculated by using different equations in theoretical modeling.

**Keywords:** Gadolinium Barium Calcium Copper Oxide(GBCCO), XRD, SEM, EDX, Debye Scherrer's formula, Young's modulus, Theoretical modeling.

## 1. Introduction

The growth of ceramics is an important qualitative change in recent decades, based on deeper scientific understanding of the composition-structure-property correlations of ceramics. Ceramics is one of the oldest technologies, with a history of about 10,000 years behind our time. The word "Ceramics" comes from Keramos, the ancient Greek word for objects made of fired clay. Today, ceramics may be defined as a product manufactured by the heat treatment of a material (or mixture of materials) which are inorganic and non-metallic<sup>1</sup>. Ceramic materials showing ferroelectric and superconducting behavior are being used in many device applications in electronics and optics. Many advantages are foreseen by the use of the majority of ceramic devices in multilayer configurations and so a good amount of work is expected in the development of newer innovative processing and fabrication techniques to improve the device performance and reduce the cost of production<sup>2-4</sup>.

In spite of their chemical inertness, high temperature stability and abundance, ceramics have always been disqualified for structural applications due to their poor tensile strength and brittleness. These handicaps have to be overcome by several new approaches. In the development of material science, the drive for composites stems from the fact that the desirable properties could not be obtained from single phase materials such as ceramics or polymers. The requirement of each and every purpose can be optimized by combining the most useful properties of the two phases which do not ordinarily appear together<sup>5-10</sup>. The ceramic-polymer composites are made up of an active ceramic phase embedded in a passive polymer phase. Nanocomposites are a new class of polymer materials with ultrafine phase dispersion of the order of a few nanometers, which show

very interesting properties often very different from those of conventional filled polymers<sup>11-14</sup>. Composites of polymers with particulate fillers have generated interest owing to their desirable improvement in certain properties for various applications. The performance of a composite material is strongly dependent on the combined effect of filler particle size, filler surface chemistry and volume fraction of the filler<sup>15-18</sup>. By principle polymer composite is a material created by the combination of two or more components, viz., selected filler or reinforcing agent and a compatible matrix in order to obtain specific characteristics and properties. Graded dielectrics with a wide range of dielectric properties can be prepared by using polypropylene matrices. The broader use of ceramic polymer composites as capacitors in dynamic random access memories (DRAMs) invokes an even greater interest in the family of materials. Development of electric devices working at high operating frequencies such as fast computers, cellular phones etc require a new high dielectric constant materials that combine good dielectric properties with both mechanical strength and ease of processing. In particular the high-K materials are required for making embedded capacitors for integrated electronic devices. Pure polymers are easy to process into mechanically robust components but generally suffer from low dielectric constant. On the other hand, typical high-K materials such as ferroelectric ceramics are brittle and require high temperature processing, which are often not compatible with current circuit integration technologies. The ideal solution would be high K-materials that is mechanically robust and procurable at ambient temperatures have to be incorporated with suitable polymers such as ceramic polymer composites that may combine desired properties of the components<sup>19-21</sup>.

In this paper the authors describes a method for the preparation of  $\text{GdBa}_2\text{Ca}_3\text{Cu}_4\text{O}_{10.5+\delta}$  ( $\text{GdBaCaCuO}$ ) or (GBCCO)-super conducting ceramic powder materials based on pre-calcinations of oxides and the prepared powder is mixed with polymer material to form a new polymer composite in different compositions. The results are analyzed by X-ray diffraction (XRD), SEM, EDX. The particle size was determined from XRD details of the ceramic powder material, GBCCO by Debye Scherrer formula. The SEM studies revealed that its particle size is in hundred nanometer range. The EDX spectrum of GBCCO gives the information on the elemental composition of the material. Young's modulus of the prepared polymer composites of different compositions are calculated by different equations in theoretical modeling.

## 2. Material and Methods

GBCCO has perovskite structure. The perovskite structure is adopted by many oxides that have the chemical formula  $\text{ABO}_3$ <sup>22</sup>. The representative structure of perovskite compounds is cubic, the compounds in this family may possess some distortion. The orthorhombic and tetragonal phases are most common variants. The ceramics with the chemical formula  $\text{GdBa}_2\text{Ca}_3\text{Cu}_4\text{O}_{10.5+\delta}$  are prepared by the conventional solid state reaction technique according to the molecular formula. For the prepared sample, the reagent grade chemicals of high purity (99.99%) ( $\text{Gd}_2\text{O}_3$ ), ( $\text{BaCO}_3$ ), Calcium Oxide ( $\text{CaO}$ ) and Cupric Oxide ( $\text{CuO}$ ) powders are used as the raw materials and weighed according to their molecular formula.

The powders of the required raw materials ceramics are mixed mechanically. Mechanical mixing is usually done by hand mixing in agate mortar for two weeks. Then ball milled with suitable balls to insure homogeneity for three months with daily sieving and mixing. Then the material calcined at  $900^\circ\text{C}$ . After the furnace is off, on cooling the oxygen is allowed to flow into the furnace at intervals (Oxygen Annealing). A final furnace temperature of  $900^\circ\text{C}$  is maintained for the intermediate firings. A temperature much higher than this will result in a material that is much harder to regrind. Temperatures above  $1030^\circ\text{C}$  may destroy the crystal structure.

The melt mixing technique is chosen for preparing the composites because it is a solvent free technique. By melting at high temperature, molten polypropylene can easily penetrate between filler particles which facilitate suitable mixing and allow avoiding air trapping into the composites. Consequently void free composites are obtained. Polypropylene-GdBaCaCuO composites are prepared in a machine called, Brabender Plasticorder which is a torque rheometer. The cavity for mixing in the instrument has capacity 40 grams and is fitted with two screw type rotors of variable speed rotating in opposite direction<sup>23</sup>. Filling the internal cavity completely with mixing charges ensures a constant ram pressure and a good mixing. For mixing, the temperature of internal mixer is raised to  $180^\circ\text{C}$  and introduced the calculated amount of polypropylene into the cavity. Complete melting of polymer is ensured by a constant minimum torque and reattainment of the desired cavity temperature of  $180^\circ\text{C}$ . Filler particle is then added to

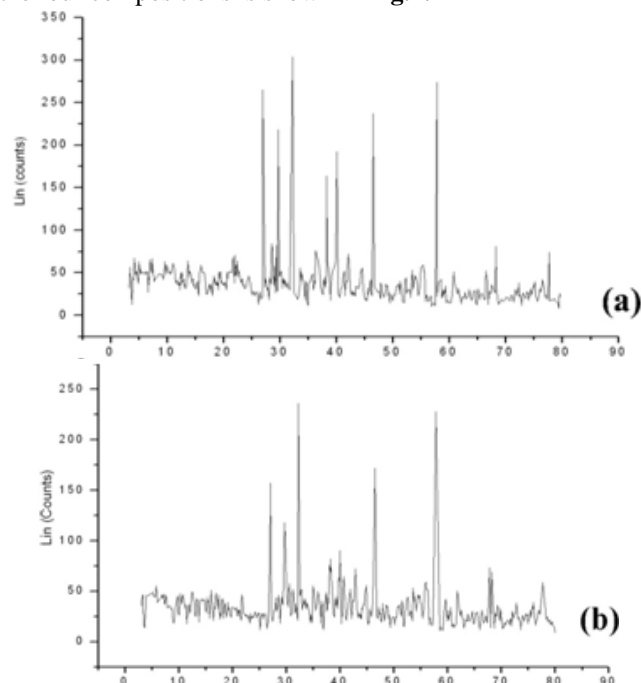
the molten polymer and mixed for about 6 minutes at a rotor speed of 60 rpm. This time is sufficient to generate a steady state torque response, indicative of uniform dispersion of the components. The compositions of the composites are 10%, 20%, 30% and 40% by the volume fraction of the filler. The mixed samples are compression molded into sheets of desired thickness by hydraulic press at a temperature of  $180^\circ\text{C}$  and are used for different studies. The composites are named as GBCCO10, GBCCO20, GBCCO30 and GBCCO40 according to their volume fraction of filling.

### 2.1 XRD Analysis

X-ray Diffraction pattern for the four compositions of the composites are taken using Bruker AXS D8 advance diffractometer. The diffractometer with radiations of wavelength  $1.54184 \text{ \AA}$  having Nickel filter, equipped with X-ray generator 1140/90/96 having X-ray source KRISTALLOFLXE 780,KF,4KE with wide angle goniometer PW1710/70 with single pen recorder pm 8203 and channel control PW1390 at 35kV, 10mA is used for the purpose. The scanning speed of the specimen is 2 degree/minute. From the XRD results, the obtained d values compared with the JCPDS (Joint Committee on Powder Diffraction Standards) file values and applied the EXPERT PRO software. So that it is found that this crystal is in orthorhombic system<sup>24</sup>:

$$a=24.6955 \text{ \AA}, b=5.4667 \text{ \AA}, c=5.1189 \text{ \AA} \quad \alpha=\beta=\gamma=90^\circ$$

Here the authors studied the change of XRD spectrum of GBCCO at different compositions of the composites. The XRD spectrum of GBCCO-polypropylene composites for the four compositions is shown in Fig.1.



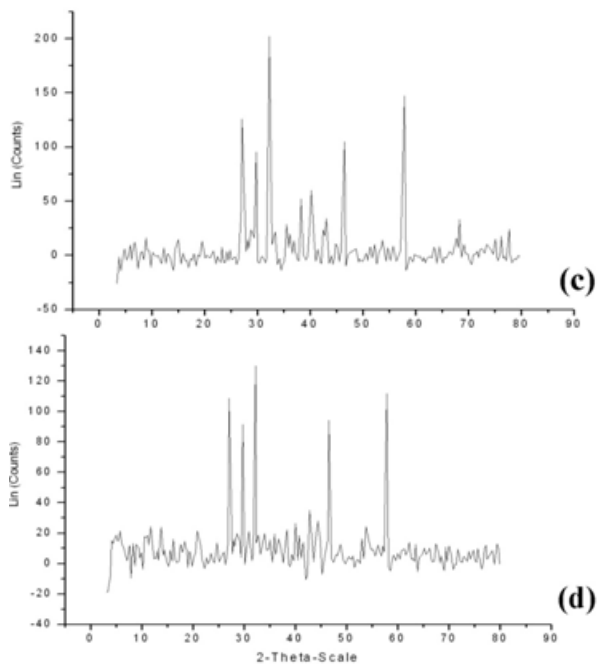


Figure 1: XRD of (a) GBCCO40, (b) GBCCO30, (c) GBCCO20 and (d) GBCCO10

## 2.2 Particle size measurements

X-ray diffraction profile may be used to measure the average crystal size in the sample provided the average diameter is less than 200Å. The lines in a powder diffraction pattern are

of finite breadth but if the particles are very small, the lines are broaden than usual. The broadening decreases with the increase in particle size. The particle size for GBCCO was calculated from X-ray diffraction profiles of strong reflections with intensity % by measuring the full width at half maximum (FWHM). The Debye Scherrer equation for calculating the particle size is given by<sup>25</sup>

$$D = \frac{K\lambda}{\beta \cos\theta}$$

Where K is the Scherrer constant,  $\lambda$  is the wavelength of light used for the diffraction,  $\beta$  is the 'full width at half maximum' of the sharp peaks and  $\theta$  is the angle measured. The Scherrer constant (K) in the above formula accounts for the shape of the particle and is generally taken to have the value 0.9.

## 2.3 SEM

Morphology has been analyzed from Scanning Electron Microscope (SEM). The SEM analyses the surface of solid objects, producing images of higher resolution than optical microscopy. It produces representations of three dimensional samples from a diverse range of materials. Fig.2 and Fig.3 are the surface morphology and fracture surface morphology of GBCCO respectively. The particle size measurement through SEM reveals its maximum dimensions always less than 100nm.

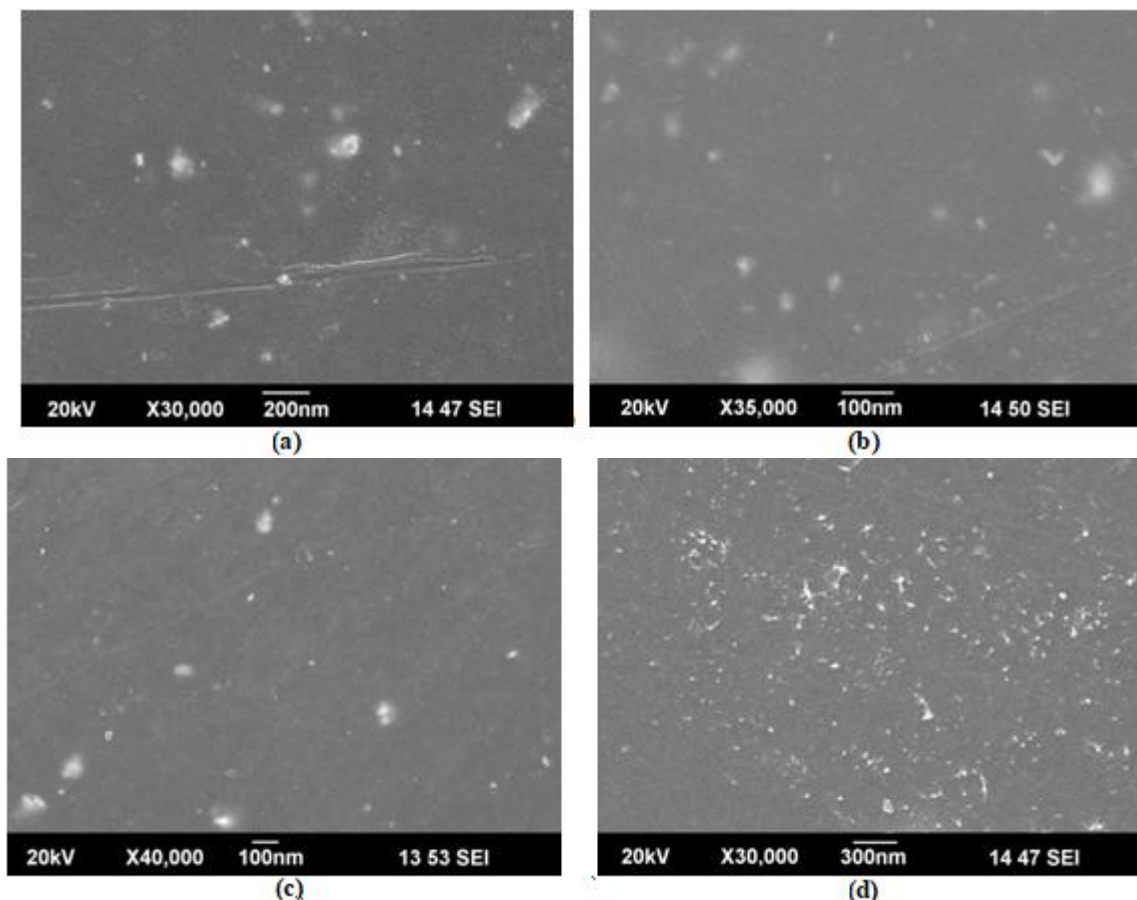


Figure 2: Surface view of (a) GBCCO10, (b) GBCCO20, (c) GBCCO30 and (d) GBCCO40

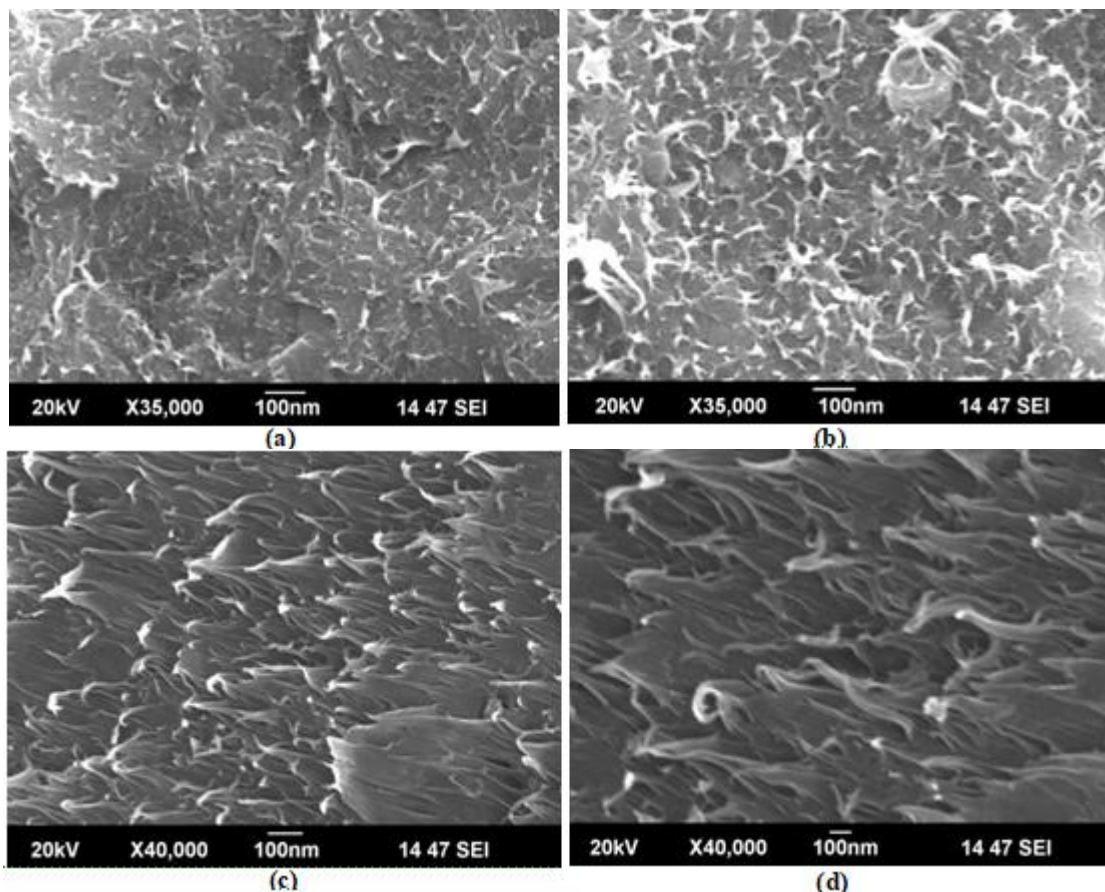


Figure 3: Fracture surface view of (a) GBCCO10, (b) GBCCO20, (c) GBCCO30 and (d) GBCCO40

#### 2.4 Energy Dispersed X-ray Spectrograph (EDX)

EDX shows the composition details of the prepared ceramic powders (Fig.4). The instrument used for this measurement is ISIS Link Oxford Instrument UK. This technique generally associated with Scanning Electron Microscope (SEM). In this technique an electron beam of 10-20 KeV strikes the surface of a sample which causes X-ray to be emitted from point of incidence. The energy of the X-ray emitted depends on material under examination. The energy of the characteristic X-ray emitted from the different elements is different and thus it gives the unavoidable

signature of the particular element. When an X-ray strikes the detector, it will generate a photoelectron which in turn generates electron-hole pairs. A strong electric field attracts the electrons and holes towards the opposite ends of the detector. The size of the pulse thus generated depends on the number electron-hole pairs created, which in turn depends on the energy of the incoming X-ray. In this method however elements with low atomic number are difficult to be detected. The detector which is lithium doped silicon (SiLi) is protected by a beryllium window and operated at liquid nitrogen temperatures. The absorption of the soft X-rays by the beryllium decreases the sensitivity below an atomic number of 11.

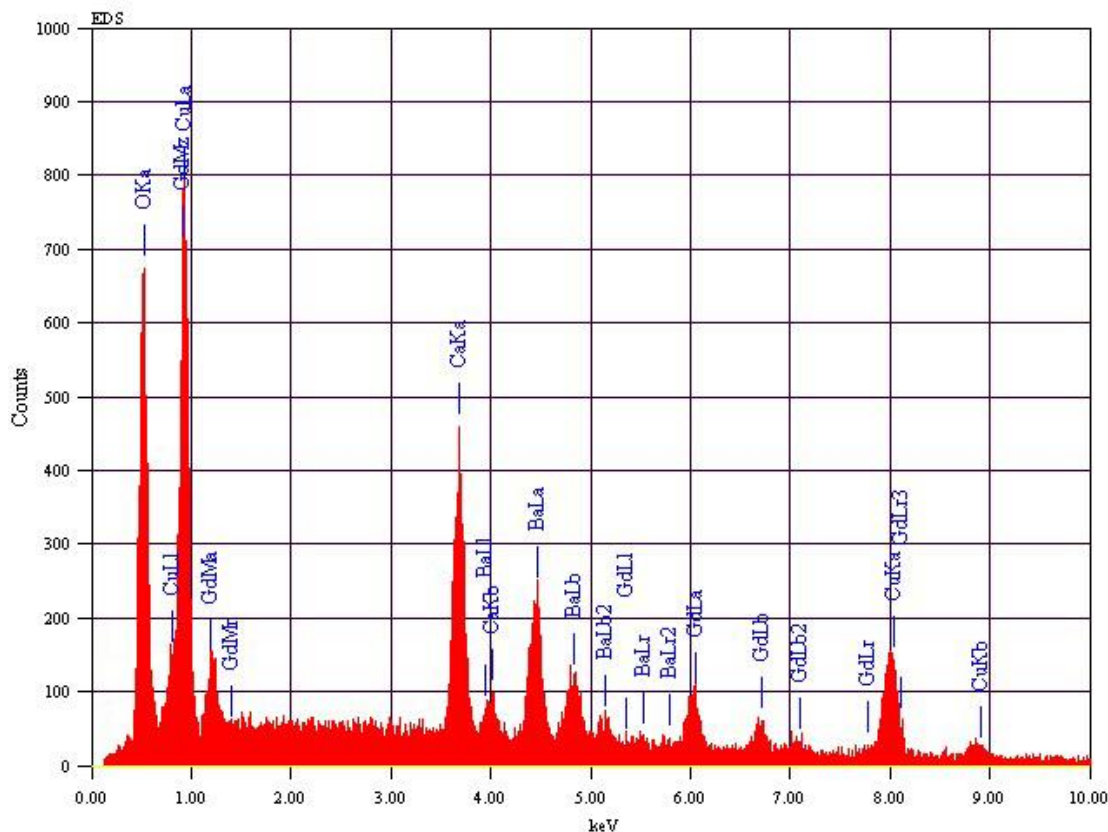


Figure 4: EDX of GBCCO

### 3. Theory

#### 3.1 Theoretical modeling

The mechanical properties of two-phase composites made up of particulate filled polymer phase have been studied in great detail. The modeling and simulation of polymer based composites has become an important topic in recent times because of the need for the development of these materials for engineering applications<sup>26</sup>. The mechanical properties of particulate filled composites are affected by a number of parameters such as filler orientation, particle size of the filler and filler/ matrix adhesion etc. Several theories have been proposed to model the Young's modulus of the non-interactive composite materials in terms of different parameters. Among the most prominent, historically and technically are those developed by Einstein<sup>27</sup>, Guth<sup>28</sup>, Quemeda<sup>29</sup>, Thomas<sup>30</sup>, Kerner<sup>31</sup> and Sato and Furukawa<sup>32</sup>. These theoretical predictions are graphically represented in Fig.5 and Fig. 6.

##### (1) Einstein equation

According to Einstein equation,

$$E_c = E_m(1 + 1.25\xi_p)$$

where  $E_c$  and  $E_m$  are the Young's modulus of composite and matrix, respectively and  $\xi_p$  is the mass ratio of the particle given by the equation,

$$\xi_p = \frac{m_p}{m_m + m_p}$$

Where  $m_m$  and  $m_p$  are the mass of the matrix and mass of the particle respectively. Einstein's equation is applicable only for materials filled with low concentrations of non interactive fillers. The equation also assumes that the filler is denser than the polymer matrix.

##### (2) Guth equation

According to Guth equation,

$$E_c = E_m(1 + 2.5\xi_p + 14.1\xi_p^2)$$

where  $E_c$  and  $E_m$  are the Young's modulus of composite and matrix, respectively and  $\xi_p$  is the mass ratio of the particle. Guth's equation is an expansion of Einstein, to account for the interparticle interactions at higher filler concentrations.

##### (3) Quemeda equation

According to Quemeda equation,

$$E_c = E_m \frac{1}{(1 - 0.5k\xi_p^2)}$$

where  $E_c$  and  $E_m$  are the Young's modulus of composite and matrix, respectively and  $\xi_p$  is the mass ratio of the particle.  $k$  is a constant normally 2 for non-interactive fillers. This variable coefficient is introduced to account for the interparticle interactions and difference in particle geometry.

##### (4) Thomas equation

According to Thomas equation,

$$E_c = E_m\{1 + 2.5\xi_p + 10.05\xi_p^2 + 0.00273\exp(16.6\xi_p)\}$$

where  $E_c$  and  $E_m$  are the Young's modulus of composite and matrix, respectively and  $\xi_p$  is the mass ratio of the particle. Thomas equation is an empirical relationship based on the data generated with dispersed spherical particles in polymer matrices.

##### (5) Kerner equation

According to Kerner equation,

$$E_c = E_m \left[ 1 + \frac{15\xi_p(1-r)}{(1-\xi_p)(8-10r)} \right]$$

where  $E_c$  and  $E_m$  are the Young's modulus of composite

and matrix, respectively  $\xi_p$  is the mass ratio of the particle and  $r$  is the Poisson's ratio of the matrix. For expansible polymers incorporating rigid spherical particles featuring some adhesion, the Kerner equation can be used to estimate the modulus.

#### (6) Sato and Furukawa equation

Sato and Furukawa have developed an expression for the modulus for the case where the adhesion is termed as the main parameter, the equation is,

$$E_c = E_m \left[ \left( 1 + \frac{\xi_p^{2/3}}{2 - 2\xi_p^{1/3}} \right) (1 - \psi j) - \frac{\xi_p^{2/3} \psi j}{(1 - \xi_p^{1/3}) \xi_p} \right]$$

Where,  $\psi = \left( \frac{\xi_p}{3} \right)^{1 + \frac{\xi_p^{1/3} - \xi_p^{2/3}}{1 - \xi_p^{1/3} + \xi_p^{2/3}}}$ ,  $E_c$  and  $E_m$  are the Young's

modulus of composite and matrix, respectively  $\xi_p$  is the mass ratio of the particle and  $j$  is the adhesion parameter,  $j=1$  for poor adhesion,  $j=0.5$  for medium adhesion and  $j=0$  for perfect adhesion.

## 4. Results and Discussion

The XRD patterns of polymer composites of GBCCO obtained for various compositions of filler and matrix are shown in **Fig.1**. The emergence of characteristic diffraction lines and their gradual sharpening increased with filler content and for the last composite GBCCO40, almost all the characteristic peaks of GBCCO are present. It is confirmed that the fillers did not react with the polymer<sup>33</sup>. The chemical non reactivity of the filler and the polymer at the processing temperature is another important factor in the preparation process. It is found that the composites showed no extra intensities due to the formation of impurity phases, but only the characteristic peaks of the fillers. This revealed that GBCCO showed no chemical reaction with polypropylene. Characterization of the composites by XRD allows identification of the crystalline components. The lattice parameters of the constituent phases are the same in all composites. The average particle size is estimated from these XRD lines, by Scherrer's equation and no noticeable change in particle size is observed. The results revealed that the particle size is 22.72 i.e., less than 100 nm. All the peaks of the composites are identified. No other additional peak is observed apart from the parent material. This confirms the successful preparation of the two-phase composite material. The humps in the diffraction pattern characterize the amorphous nature of polypropylene. They gradually gave way to discrete lines with the increment in filler content. It is observed that the characteristic peaks with high intensity are found to increase with increasing proportion of the filler.

**Fig.2 & Fig.3** showed SEM image of GBCCO polymer composites for various compositions. The SEM photograph revealed maximum dimensions of the particles to be always less than 100nm. This is an experimental proof of the theoretical calculation of particle size by Debye Scherrer equation from XRD data. SEM analysis supported the reinforcement of fillers in the composites. The filler particles are uniformly distributed in all the composites and the particles are almost spherical in shape with irregular boundaries. The results give a true picture of how the fillers interact with polypropylene matrix that effect the overall

properties of the composites. The most fascinating property is the uniform dispersion of the fillers in the matrix. The surface view and fracture surface view of GBCCO-polypropylene composites revealed the dispersion of the particles in the composites (**Fig.2&Fig.3**). The particle dispersion and particle-matrix reinforcement play vital roles for both tensile and elongation properties of the composites. The ceramic particles are dispersed homogeneously with the interspaces filled with polypropylene, and large defects are not observed in the fracture surface view of the composites<sup>34</sup>. The fractured surface of the composites showed a dense microstructure as in **Fig.3(a-d)**. SEM photographs are used to determine the size of the dispersed particle and the particle size distribution.

**Fig.4** shows EDX spectrum of GBCCO. The EDX spectrum of GBCCO gave the information on the elemental composition of the material. This technique is generally associated with SEM. The percent of the elemental composition as in **Table.1** agrees with the stoichiometric relations of  $GdBa_2Ca_3Cu_4O_{10.5+\delta}$ . From the EDX spectrum, the five dominant peak positions at 6.056keV, 4.465keV, 3.69keV, 8.04keV, 0.525keV correspond quite well to the energy pattern of the corresponding materials (Gd, Ba, Ca, Cu, and O) reported in the EDAX international chart, giving the evidence that Gd, Ba and Cu are dominant in GBCCO samples.

**Table 1:** Material Content of  $GdBa_2Ca_3Cu_4O_{10.5+\delta}$  from EDX

Material	Content (%)
Gd	16.55
Ba	30.30
Ca	14.44
Cu	23.94
O	14.77

The mechanical properties such as Young's modulus of two-phase composites made up of particulate filled polymer phase have been studied in great detail by using different equations. It can be seen that in most conventionally filled polymer systems the modulus increases linearly with the filler volume fraction as shown in the **Fig.5**. The increase of modulus is mainly governed by the particle size of the filler. The explanation is based on the assumption of a special morphology of the polymer matrix around the filler particles. When a thermoplastic is cooled down from the melt a solidification process will take place. During cooling from the processing temperature of the composites (180°C) to room temperature the filler particles are assumed to act as sites where thermal contraction is particularly favored, which should cause the special morphology. Figure 6 shows the Theoretical modeling of the tensile modulus of GBCCO-different volume fraction- filled polypropylene composites with different adhesion parameters. If it is assumed that the polymer adjacent to the embedded particles contract in an earlier stage of process because of the difference in thermal conductivity of the polymer (0.1–0.2 W/m/K) and that of ceramics is (~1– 40 W/m/K), a zone with a higher density (high modulus) will be formed around the filler particle. Because of the heat transportation processes, a depletion zone with relatively low density (low modulus) will be created surrounding the high-density zone. It is essentially

due to the different thermal expansion of polymer ( $50 \times 10^{-6} \text{K}^{-1}$  to  $300 \times 10^{-6} \text{K}^{-1}$ ) on one hand and ceramics ( $0.5 \times 10^{-6} \text{K}^{-1}$  to  $15 \times 10^{-6} \text{K}^{-1}$ ) on the other hand<sup>35</sup>.

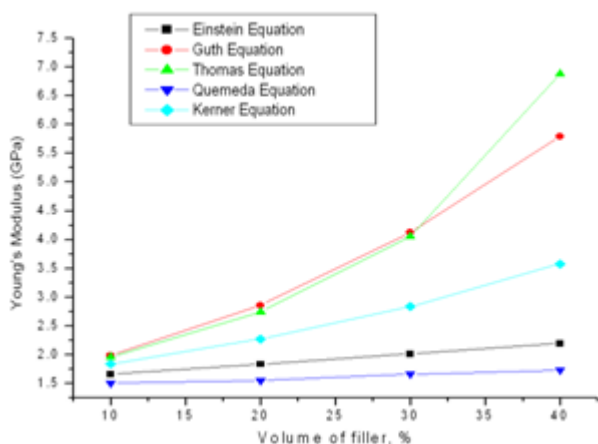


Figure 5: Theoretical modeling of the tensile modulus of GBCCO (different volume fraction) filled polypropylene composites

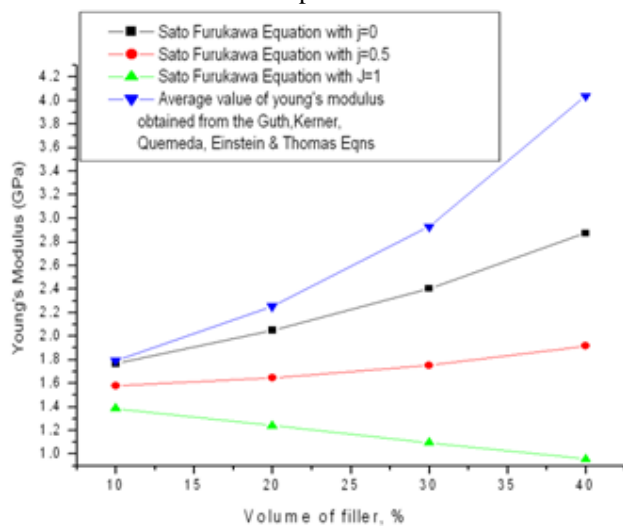


Figure 6: Theoretical modeling of the tensile modulus of GBCCO-different volume fraction- filled polypropylene composites with different adhesion parameters

According to Van Krevelan<sup>36</sup> Young's modulus(E) is proportional to the seventh power of density( $\rho$ ). This means that the starting zones, which have a higher density, have a higher Young's modulus, and the depletion zones, which have a lower density, have a lower modulus. The filler particles can act as initiation sites of the solidification process, and for this reason they could be surrounded by an enriched layer of polymer with an increased modulus (high modulus layer), around which a zone of material with a lower modulus is found<sup>37</sup>. The effect of this morphology on the Young's modulus of the filled polymer with respect to the filler particle size will cause a combination of both effects. Two extremes are treated: a polymer filled with very small particle (nano particle), and a polymer filled with very large particles ( $\text{size} > 10\mu\text{m}$ ). Of course, an intermediate particle size will cause a combination of both effects. In the case of composite material filled with nano particles, the interparticle distance is so small and by the abundance of number of particles there is a huge number of starting points for thermal contraction process, so that a homogeneous

matrix material of 'high modulus' polymer is assumed to be created around the filler particle (Fig.7&Fig.8). For a large filler particle the thickness of high modulus layer is very small compared to the diameter of the filler particle. With Sato and Furukawa relations, Young's modulus can be calculated with an adhesion parameter  $j = 1$  for poor adhesion,  $j = 0.5$  for medium adhesion, and  $j = 0$  for good adhesion. The data for various volume fractions of GBCCO is found to be less than that with the case of  $j = 1$  and the results obtained with adhesion parameter  $j=0$  are fully satisfied as in Fig.6. This type of perfect adhesion is due to the formation of the high modulus layer around the GBCCO particles.

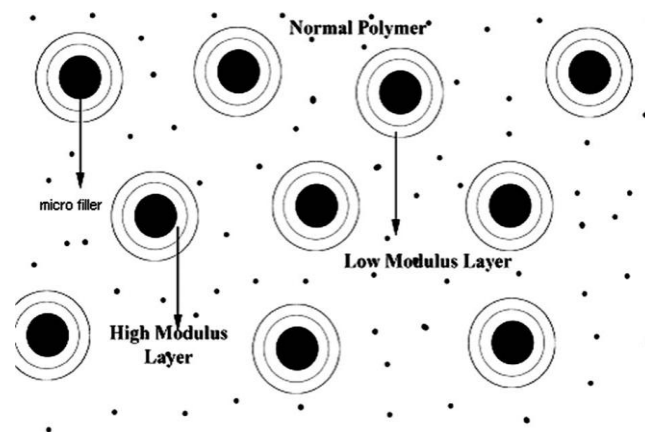


Figure 7: Proposed morphology of the polymer matrix with micro size filler particles.

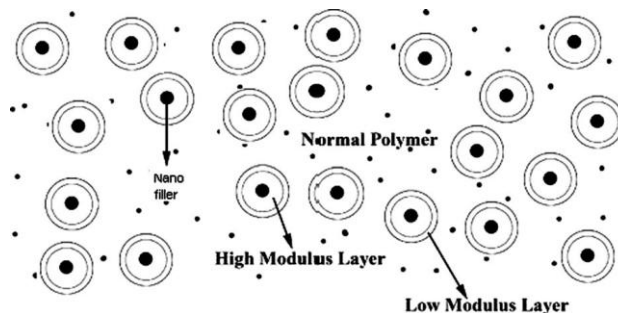


Figure 8: Proposed morphology of the polymer matrix with nano size filler particles

From the above discussions it could be argued that the particle size play an important role in Young's modulus value. Generally, the elastic modulus increases with augmenting filler volume fraction, while all other tensile properties such as the ultimate stress and strain at break decreases with increasing filler volume fraction<sup>38</sup>. However, many investigations showed that the effect of solid fillers on the tensile strength of polymers might be positive or negative, depending on such factors as filler size and shape, internal stresses, surface nature, and aspect ratio. In the prepared composites, the interaction between filler and polymer is expected to be physical. The polymer matrix is, however, stiffened by the particulate. The particles restrict the mobility and deformability of the matrix by introducing a mechanical restraint, the degree of which depends on the particulate spacing and the properties of the particle and the matrix. Restriction in polymer molecular diffusion is seen in the presence of solid particles. The most important feature that affects the interfacial adhesion is believed to be the

mechanical stresses, chemical interactions, and physico-chemical weak boundary layers.

## 5. Conclusion

In this work, GBCCO ceramics are prepared successfully by the conventional solid state reaction technique and polypropylene composites are prepared by the melt mixing technique. The composites are prepared for different compositions and analyzed by XRD, SEM and EDX. The mechanical properties such as Young's modulus of two-phase composites are calculated using different equations in theoretical modeling and plotted graphically.

SEM results revealed a true picture of how the fillers interact with polypropylene matrix that affects the overall properties of the composites. In all composites filler particles are clearly embedded in the polymer matrix. The surface view and fracture surface view of GBCCO –polypropylene composites revealed the dispersion of the particles in the composites. The EDX analysis indicates that the elements existing in the sample and it agree with the stoichiometric relations of the prepared compound. Theoretical modeling for calculating Young's modulus of the different compositions of composites revealed that the value of Young's modulus increases with the filler volume fraction.

## 6. Acknowledgement

The authors are thankful to Kerala State Council for Science, Technology and Environment (KSCSTE), Thiruvananthapuram for granting the financial assistance, SAIF, Kochi for providing the data analysis and to the Principal, CMS College, Kottayam, Kerala for providing the facilities.

## References

- [1] Kittel, C. Introduction to Solid state Physics. John Wiley & Sons, 1997.
- [2] Chang, B.Y.; Seung, H. L.; Sung, M. L.; Young, H. K.; Hyoun, E. K.; Kyung, W. L. Piezoelectric Multilayer Ceramic/Polymer Composite Transducer with 2–2 Connectivity. *J. Am. Ceram. Soc.* 2006, 89, 2509–2513. DOI: 10.1111/j.1551-2916.2006.01080.x
- [3] Saigal, A.; Giannakopoulos, A. E.; Petteermann, H. E.; Suresh, S. Electrical response during indentation of a 1-3 Piezoelectric Ceramic-polymer composite. *J. Appl. Phys.* 1999, 86, 603 – 606. DOI: 10.1063/1.370773
- [4] Asit, B. P.; Amita, P.; Panchanan, P. Low temperature preparation of Nanocrystalline solid solution of Strontium–Barium–Niobate by chemical process. *Mater. Lett.* 2002, 52, 180–186. DOI: 10.1016/S0167-577X(01)00389-5
- [5] Mitsui, T; Tatsuzaki, I; Nakamura, E. An Introduction to the Physics of Ferroelectrics. Gordon and Breach Publishers: London, 1976.
- [6] Cross, L. E. Relaxor Ferroelectrics. *Ferroelectrics.* 1987, 76, 241-267. DOI: 10.1080/00150198708016945
- [7] Bhatnagar, M. S., Dr. Chemistry and Technology of Polymers. S Chand: New Delhi, 2004.

- [8] Joel, R. F. Polymer Science and Technology. Prentice Hall: New Delhi, 2000.
- [9] Acharya, H.; Srivastava, S. K.; Bhowmick, A. K. Ethylene propylene diene terpolymer/ethylene vinyl acetate/layered silicate ternary nanocomposite by solution method. *Polym. Eng. Sci.* 2006, 46, 837–843. DOI: 10.1002/pen.20537
- [10] Wang, H. W.; Chang, K. C.; Chu, H. C.; Liou, S. J.; Yeh, J. M. Significant decreased dielectric constant and loss of polystyrene–clay nanocomposite materials by using long-chain intercalation agent. *J. Appl. Polym. Sci.* 2004, 92, 2402–2410. DOI: 10.1002/app.20192
- [11] Emmanuel, P. G., Prof. Polymer Layered Silicate Nanocomposites. *Adv. Mater.* 1996, 8, 29–35. DOI: 10.1002/adma.19960080104
- [12] Wu, Y. P.; Zhang, L. Q.; Wang, Y. Q.; Liang, Y.; Yu, D. S. Structure of Carboxylated Acrylonitrile-butadiene Rubber (CNBR)–clay Nanocomposites by co-coagulating rubber latex and clay Aqueous suspension. *J. Appl. Polym. Sci.* 2001, 82, 2842–2848. DOI: 10.1002/app.2138
- [13] Ramanan, K.; Richard, A. V.; Emmanuel, P. G. Structure and Dynamics of Polymer-Layered Silicate Nanocomposites. *Chem. Mater.* 1996, 8, 1728–1734. DOI: 10.1021/cm960127g
- [14] Marco, Z.; Sergei, L.; Giovanni, C. Polymer layered Silicate Nanocomposites. *Macromolecular Materials and Engineering* 2000, 279, 1–9. DOI: 10.1002/1439-2054(20000601)279:1<1::AID-MAME1>3.0.CO;2-Q
- [15] Wu, A.; Vilarinho, P. M.; Kholkin, A. Low Temperature Preparation of Ferroelectric Relaxor Composite Thick Films. *J. Am. Ceram. Soc.* 2007, 90, 1029–1037. DOI: 10.1111/j.1551-2916.2007.01587.x
- [16] Bai, S. L.; Chen, J. K.; Huang, Z. P.; Liu, Z. D. Interface effect on the mechanical behavior of rigid particle filled polymer. *Polym. Int.* 2001, 50, 222–228. DOI: 10.1002/1097-0126(200102)50:2<222::AID-PI609>3.0.CO;2-H
- [17] Cowie, J. M. G. Polymers: Chemistry & Physics of Modern Materials. Chapman & Hall, 1991.
- [18] James, E. S.; Joseph, C., III.; Bruce, A. T.; Jennifer, A. L. Piezoelectric properties of 3-X periodic Pb (ZrxTi1-x) O3–polymer composites. *J. Appl. Phys.* 2002, 92, 6119. DOI: 10.1063/1.1513202
- [19] Pillai, S. O. Solid State Physics. New age international: New Delhi, 1996.
- [20] Barranco, A. P.; Martinez, O. P. Piezo-, pyro-, ferroelectric, and dielectric properties of (Pb0.88Sm0.08)(Ti1-xMnx)O3/ poly ether ketone 50/50vol % ceramic/polymer composites. *J. Appl. Phys.* 2002, 92, 1494 – 1499. DOI: 10.1063/1.1490615
- [21] Kingery, W. D; Bowen, H. K; Uhlmann, D. R. Introduction to Ceramics. John Wiley & Sons, 1995.
- [22] Galasso, F. S. Structure, Properties and Preparation of Perovskite Type Compounds. Pergamon Press: Oxford, 1969.
- [23] Selvin, P. T.; Joseph, K.; Sabu, T. Mechanical properties of Titanium dioxide-filled Polystyrene microcomposites. *Mater. Lett.* 2004, 58, 281–289. [http://dx.doi.org/10.1016/S0167-577X\(03\)00470-1](http://dx.doi.org/10.1016/S0167-577X(03)00470-1)

- [24] V. S. Vinila, Jayakumari Isac. Investigation of Nano Crystalline Ceramic Superconductor GdBaCaCuO: Structural and Morphological Aspects. *The Journal of Physics. Photon.* 2015,110, 228-235
- [25] West, A. R. *Solid State Chemistry and its Applications.* Wiley: New York, 1974.
- [26] Alexander, B. M.; Chu, L. L.; Joseph, D. H. A. Flammability Performance Comparison between Synthetic and Natural clays in Polystyrene Nanocomposites. *Fire and Materials.*2005, 29, 213–229. DOI: 10.1002/fam.881
- [27] Smallwood, H. M. Limiting Law of the Reinforcement of Rubber. *J. Appl. Phys.*1944,15, 758-766. DOI : 10.1063/1.1707385
- [28] Guth, E. Theory of Filler Reinforcement. *J. Appl. Phys.*1945, 16, 20-25. DOI: 10.1063/1.1707495.
- [29] Quemeda, D. Rheology of concentrated disperse systems and minimum energy dissipation principle. *Rheology Acta.*1977,16, 82-94. DOI: 10.1007/BF01516932
- [30] Evelvin, D. B.; Chris, C. W.; Montgomery, T. S. Mechanical Properties of blends of HDPE and Recycled Urea-formaldehyde resin. *J. Appl. Polym. Sci.*2000,77, 3220-3227. DOI: 10.1002/1097-4628(20000929)77:14<3220::AID-APP250>3.0.CO; 2-4
- [31] Kerner, E. H. The Elastic and Thermo-elastic Properties of Composite Media. *Proceedings of the Physical Society Section B.*1956,69, 808. DOI:10.1088/0370-1301/69/8/305
- [32] Sato, Y; Furukawa, J. A. Molecular Theory of Filler Reinforcement Based upon the Conception of Internal Deformation (A Rough Approximation of the Internal Deformation). *Rubber Chemistry and Technology.*1963, 36, 1081-1106. DOI: 10.5254/1.3539632
- [33] Huang, Q. W.; Wang, P. L.; Cheng, Y. B; Yan, D. S. XRD analysis of formation of strontium barium niobate phase. *Mater. Lett.*2002,56, 915–920. [http://dx.doi.org/10.1016/S0167-577X\(02\)00637-7](http://dx.doi.org/10.1016/S0167-577X(02)00637-7)
- [34] Mao, X.; Shimai, S.; Dong, M.; Wang, S. Gelcasting of Alumina Using Epoxy Resin as a Gelling Agent. *J. Am. Ceram. Soc.*2007,90,986–988. DOI: 10.1111/j.1551-2916.2007.01492.x
- [35] Zakin, J. L.; Simha, R.; Hershey, H. C. Low-temperature thermal expansivities of polyethylene, polypropylene, mixtures of polyethylene and polypropylene, and polystyrene. *J. Appl. Polym. Sci.*1966, 10, 1455–1473. DOI: 10.1002/app.1966.070101006
- [36] Van Krevelan, D. W. *Properties of Polymers.* Elsevier: Amsterdam, 1972.
- [37] Vollenberg, P. H. T; de Haan, J. W; van de Ven, D. Heikens. Particle size dependence of the Young's modulus of filled polymers: 2. Annealing and solid-state nuclear magnetic resonance experiments. *Polymer.*1989, 30, 1663–1668. [http://dx.doi.org/10.1016/0032-3861\(89\)90327-3](http://dx.doi.org/10.1016/0032-3861(89)90327-3)
- [38] Bruneel, E.; Persyn, F.; Hoste, S. Mechanical and superconducting properties of BiPbSrCaCuO-PE and BiPbSrCaCuO-MgO composites. *Supercond. Sci. Technol.*1998,11, 88-93. DOI:10.1088/0953-2048/11/1/018.